

TRIUMF	UNIVERSITY OF ALBERTA EDMONTON, ALBERTA	
	Date 1996-10-07	File No. TRI-DNA-96-9
Author GM Stinson		Page 1 of 31
Subject A revision of the 480 MeV to 500 MeV beam transport system to a ISAC Facility		

1. Introduction

A recent reports¹⁾ gave a detailed optical design for a beam line for the delivery of beam to an external ISAC. Since that report was issued a revision of the optics of the beam line has been undertaken. The major change is relocation of the the quadrupole that in ref¹⁾ was between the two 15° dipoles to a location downstream of the last quadrupole of the beam line. At the same time, the ±15° switching magnet was replaced with a 15° rectangular magnet in order that only one design for the 15° magnets was required now. This is because only the west target—denoted TGT2 in this report—will be installed initially. Later, when installation of the east target—designated here as TGT1—is contemplated, it will be necessary to design a ±15° switching magnet of course.

Thus the section of beam line immediately upstream of the target now consists of a quadrupole doublet followed by two 15 ° rectangular dipoles and another quadrupole doublet. *No* other changes to the configuration of the beam line have been made.

This report presents a design for this new configuration.

2. Design Modification

2.1 An overview

Figure 1, taken from ref¹⁾, shows the beam line configuration that was presented in TRI-DNA-96-5. In that report it was noted that the vertical beam size at the target was affected by foil scattering. In an attempt to reduce the vertical beam size at the target the quadrupole between the two 15° dipoles was relocated downstream of the last quadrupole to form a quadrupole doublet and a double waist was required at the target location. This was relatively easily accomplished in TRANSPORT²⁾ but when REVMOC³⁾ runs were made it was found that REVMOC predicted that the vertical waist was downstream of the target. Further runs were made with TRANSPORT with a split waist—a horizontal waist at the target and a vertical waist approximately 0.9 m upstream of the target. However, with the use of two rectangular magnets a viable split-waist solution could not be found for *both* targets. Consequently, the split-waist requirement was dropped in lieu of requirements for a vertical waist approximately 0.9 m *upstream* of each target (so as to produce a vertical waist *at* each target), a spatially non-dispersed beam at each target ($R_{16} = 0$ but $R_{26} \neq 0$) and a nominal beam size at each target of $\pm x = \pm y = \pm 2.5$ mm. REVMOC runs then confirmed that there was, indeed, a vertical waist at the each target location.

Figure 2 shows the configuration of the beam line with this modification. An enlarged view of the WST4 to targets section of the beam line is shown in figure 3. As in ref¹⁾, in each of these figures, and throughout this report, element locations are specified in a Cartesian coordinate system that is located with its origin $(x_0, y_0) = (0, 0)$ at the cyclotron center. The positive x -axis is directed east and the positive y -axis is directed north.

For completeness we include the following sub-section taken directly from ref¹⁾.

2.2 Starting Point of the Beam line

Extraction parameters for beam line 2A were calculated by R. Lee⁴⁾ in October of 1995. Listed in table 1(a) are the relevant data that he has provided for the combination magnet parameters and in table 1(b) for the phase space parameters and the matrix elements for the fringe fields.

Extraction studies track the stripped beam from the stripper foil to a point well beyond the (effective) edge of the combination magnet. Consequently, it is necessary to determine that location in order to specify the location of the components of the beam line.

The upper portion of figure 4 shows the trajectories of the extracted beam as calculated by R Lee. It shows that the crossover point of the combination magnet is located at an (R, θ) coordinate of (412.32 inches, 327.00°) with respect to the centerline of valley 3. Consequently, the radius vector makes an angle of $(29^\circ + 327^\circ - 360^\circ) = -4.0^\circ$ with respect to the positive x -axis of this report. In this coordinate system then, the crossover point is located at the coordinates

$$\begin{aligned}(x_{co}, y_{co}) &= (412.32 \cos(-4.0^\circ), 412.32 \sin(-4.0^\circ)) \text{ inches} \\ &= (411.315609, -28.761989) \text{ inches} \\ &= (10.447417, -0.730555) \text{ m.}\end{aligned}$$

Recalling that the effective length of the magnet has been taken as 13.78 inches (0.35 m) and assuming that the crossover point is at the center of the magnet, we then calculate the distance from there to the magnet edge as

$$\begin{aligned}(\delta x, \delta y) &= (6.89 \cos(35.0^\circ), 6.89 \sin(35.0^\circ)) \text{ inches} \\ &= (5.643958, 3.951942) \text{ inches} \\ &= (0.143357, 0.100379) \text{ m.}\end{aligned}$$

Thus the exit edge of the magnet is located at

$$\begin{aligned}x_{magexit} &= x_{co} + \delta x \\ &= 10.447417 + 0.143357 \text{ m} \\ &= 10.590774 \text{ m}\end{aligned}$$

and

$$\begin{aligned}y_{magexit} &= y_{co} + \delta y \\ &= -0.730555 + 0.100379 \text{ m} \\ &= -0.630176 \text{ m.}\end{aligned}$$

From the work of R. Lee we find that at 489.466 MeV the tracing done to generate the fringe-field transfer matrices ends at an $(R_{traj}, \theta_{traj}) = (436.345 \text{ inches}, 329.511^\circ)$. Thus, in the (x, y) system used here, the extracted trajectory makes an angle with respect to the positive x -axis of $(29^\circ + 329.511^\circ - 360^\circ) = -1.489^\circ$ and the end of the fringe-field calculation becomes

$$\begin{aligned}(x_{traj}, y_{traj}) &= (436.345 \cos(-1.489^\circ), 436.345 \sin(-1.489^\circ)) \text{ inches} \\ &= (436.197660, -11.338437) \text{ inches} \\ &= (11.079421, -0.287996) \text{ m.}\end{aligned}$$

Thus we must back up a distance

$$\begin{aligned}\Delta_{490} &= \sqrt{(x_{traj} - x_{magexit})^2 + (y_{traj} - y_{magexit})^2} \\ &= \sqrt{(11.079421 - 10.590774)^2 + (-0.287996 - (-0.630176))^2} \\ &= \sqrt{0.488647^2 + 0.342180^2} \\ &= 0.596543 \text{ m}\end{aligned}$$

along the exiting trajectory to reach the magnet exit. Similar calculations at an energy of 499.456 MeV [end-point $(R_{traj}, \theta_{traj}) = (436.169 \text{ in.}, 329.493^\circ)$] and 479.477 MeV [end-point $(R_{traj}, \theta_{traj}) = (436.498 \text{ in.},$

$329.526^\circ]$] yield values of $\Delta_{500} = 0.590696$ m and $\Delta_{480} = 0.601392$ m respectively. We average these to obtain the average back-up distance

$$\Delta_{av} = 0.596210 \text{ m.}$$

In the TRANSPORT calculations presented here, a back-up distance of 0.59617 m was used (in error). However, the 0.4 mm error introduced will have no effect on the calculations.

3. Beam Line Design

3.1 General Considerations

Because there has been no change in the beam optics upstream of the WST4 location, the design philosophy followed in ref¹⁾ was maintained. For completeness, we summarize below the optics of the beam line as given in that reference. Ref¹⁾ should be consulted for more details of the optical design and for beam profiles in the sections upstream of the WST4 location.

In the cyclotron vault, a quadrupole doublet located downstream of the combination magnet and upstream of the first of two 27.5° dipoles and a second doublet positioned downstream of the second dipole are used to control the vertical beam height in the dipoles and to produce a double waist at the point labelled WST1. In addition, a beam size of $(\pm x, \pm y) = (\pm 1.1, \pm 0.66)$ cm is required at the waist.

The first doublet is composed of two of the standard TRIUMF 4Q14/8 quadrupoles. Those of the second doublet are of a new TRIUMF design^{5,6)}, modified as suggested by A. Otter⁷⁾, and are akin to the TRIUMF 4Q9/8 quadrupoles that were purchased from Alpha Magnetics some time ago. These new quadrupoles are designated as TRIUMF type 4Q8.5/8.

The section of beam line from the WST1 to the WST3 locations carries the beam through the vault wall and into the 2A tunnel. It consists of the triplet 2AVQ5/6/7 of 4Q8.5/8.5 quadrupoles just inside the north wall of the vault followed by the 2AQ8/9/10 triplet of 4Q14/8 quadrupoles. The first triplet produces a double waist at the position labelled WST2, 8 m from the external wall of the vault. The second triplet produces another waist at the location labelled WST3. These two triplets are tuned to keep the vertical size of the beam small and to produce a vertical beam size of ± 0.29 cm at WST3.

The section of beam line between the WST3 and WST4 locations is composed of the quadrupole doublet 2AQ11/12. Quadrupoles of the 4Q6.5/8.5 type are used to produce another double waist at the WST4 location.

3.2 The WST4 to target section

This section of beam line consists of the two quadrupole doublets 2AQ13/14 and 2AQ15/16, and two 15° rectangular dipole magnets 2AB3 and 2AB4. All of the quadrupoles are of the 4Q8.5/8.5 variety. These quadrupoles are used to produce the required beam size at the target location and, at the same time, to produce a vertical waist approximately 1 m upstream of the target and a spatially achromatic beam spot ($R_{16} = 0, R_{26} \neq 0$) at the target.

The difference between this configuration and that of ref¹⁾ is in the relocation of quadrupole 2AQ15 from between the two 15° dipoles as in ref¹⁾ to downstream of quadrupole 2AQ16 in this new configuration. Further, in order that only one additional dipole type be designed now, the $\pm 15^\circ$ switching magnet has been replaced with a rectangular 15° dipole of the same type that lies upstream of the target.

A TRANSPORT listing for delivery of a 500 MeV beam to the west target (TGT2) case is given in table 2. Figure 5 shows the beam envelopes along the beam line for beam delivery to the TGT2 target. Only profiles for 490 and 500 MeV are shown because the 480 MeV envelopes are indistinguishable from those of the 490 MeV tune. (In future plots of beam envelopes, this procedure will be maintained.) The small

'tail' that appears in this plot at the beginning of the beam line results because of the back up to the effective exit of the combination magnet that is required. Figure 6 shows an enlargement of the beam profiles in the WST4 to TGT2 and TGT1 sections of the beam line. We again note that in each of the figures the cyclotron center is taken as $(x, y) = (0,0)$.

Beam profiles and an expanded view of this section of beam line are shown figure 7. A nominal beam size at the target of $(\pm x, \pm y) = (\pm 0.25, \pm 0.25)$ cm was the design goal.

4. Settings of the beam-transport elements

Table 3 lists the settings of the various elements of the transport system for the energy range 480, 490 and 500 MeV. In table 4 we list the beam sizes at the various waist locations.

Beam sizes and overall transfer matrices at the TGT2 location are listed in table 5(a); those at the TGT1 location are listed in table 5(b).

5. REVMOC calculations

The program REVMOC⁷⁾ was run at all energies to estimate the amount of beam spill to be expected and where such might occur. REVMOC is a Monte Carlo program that traces particles through a beam optics configuration using true second-order optics, although the effects of chromatic aberrations is considered to all orders. The effects of multiple scattering, decay, nuclear scattering and energy loss in scatterers, absorbers, collimators, slits and apertures are included. Geometric effects are considered locally to only second order but higher-order global effects will appear because of the accumulation of the second-order effects. The program does not, however, optimize beam elements and its primary use is to do detailed checks on a beam line that has been designed using the program TRANSPORT⁸⁾.

For each energy and each target configuration 150,000 particles (in some cases, 1,500,000 particles) were traced through the beam line. At 500 and 490 MeV a spill of 0.0094% of the beam was predicted to be lost between the stripper foil and the combination magnet exit; at 480 MeV a spill of 0.0093% was predicted in the same region. No beam was predicted to be spilled elsewhere in the beam line. All spill was predicted to occur in the vertical plane.

The reason for spill in the vertical plane only is shown in figure 8, a plot of the vertical divergence (DY) in mr along the vertical axis versus the vertical beam size (Y) in cm along the horizontal axis at the WST1 location. The upper portion of the plot is a prediction of this correlation *without* any foil scattering taken into account; the lower portion is the prediction taking into account the scattering in a carbon stripper foil that is 0.00003 m (0.0012 in.) thick. It is clear that the foil scattering adds significantly to the beam divergence. The reason for this, as discussed in section 3.1, is the extremely low vertical divergence of the beam at the point of stripping.

Figure 9 shows the predicted beam spot at the TGT2 target location for a beam energy of 500 MeV. The spot size shown includes the effect of foil scattering. The units of the vertical and horizontal scales are cm. Figure 10 is a plot of the predicted beam spot at the TGT1 location.

Figures 11 and 12 are similar plots for a beam energy of 490 MeV and figures 13 and 14 those for a beam energy of 480 MeV.

Using the data presented in figure 9, we find that REVMOC predicts that 3.55% (2.60%) of the beam lies *outside* the nominal design spot size of ± 0.26 cm in the horizontal (vertical) plane at a beam energy of 500 MeV. From figure 10 we see that 4.07% (2.21%) of the beam lies outside of these nominal dimensions. At 490 MeV we find the corresponding values of percentages of beam outside the nominal design values are 3.39% (2.58%) for the horizontal (vertical) plane at TGT2 and 4.07% (2.21%) for the horizontal (vertical) plane

at TGT1. At 480 MeV the percentage of beam outside of the nominal design values are 3.38% (2.98 %) for the horizontal (vertical) plane at TGT2 and 4.05% (1.87%) for the horizontal (vertical) plane at TGT1.

Finally, figure 15 shows a plot of momentum p in GeV/c along the vertical axis versus horizontal position x in cm along the horizontal axis at the TGT2 location. That momentum and horizontal position are uncorrelated indicates that the beam is spatially achromatic there. Similar plots for 490 and 480 MeV show the same property.

6. The effect of a window at the end of the beam line

Subsequent to the issue of ref¹⁾ it was pointed out to the author that a window was required upstream of the target to provide separation of the beam line and cyclotron vacuum systems from the relatively poor and possibly dirty vacuum of the target enclosure. Because of this a study of the effect of such a window on the beam size at the target was undertaken.

The program REVMOC was again used to find the effect of a 0.001 in. thick, stainless steel window at various locations upstream of the targets. In a series of runs, windows were placed 1.0, 1.5 and 2 m upstream of the TGT2 target and their effect on the beam spot at the target examined. These runs were made only at 500 MeV and for the TGT2 location on the assumption that similar effects would be observed at the other energies and at the TGT1 location.

As would be expected, this study showed that the closer to the target the window was, the less the effect on beam size there. The most practical location for a window is approximately 1 m upstream of the target. Figure 16, drawn to the same scales as figure 9, shows the predicted beam size at the TGT2 location with both foil and window scatterings included for such a case. A comparison of the data presented in figures 9 and 16 is useful.

The effect of the window is to increase significantly the percentage of beam outside of the design goal of ± 2.5 mm in each plane. With the window in place, 6.91% of the beam in the horizontal plane and 5.88% of the beam in the vertical plane lies outside of the nominal dimensions. This is roughly twice the percentages lying outside of the design values that are predicted to occur with no window. On the other hand, only 0.92% of the beam lies beyond values of $x = \pm 3.6$ mm in the horizontal plane and 0.57% of the beam lies beyond values of $y = \pm 3.8$ mm in the vertical plane. Thus, in a sense, the introduction of the window symmetrizes the beam at the expense of an increase of 2 mm in the beam size in each of the horizontal and vertical planes.

7. Discussion

Since a proposal for an ISAC facility was first made, many versions of its beam transport line have been considered. This report presents the results of a revision of the beam line design presented in ref¹⁾.

Extraction matrices have been produced for energies of 480, 490 and 500 MeV and beam-line optics for these energies have been developed. In addition, beam spill calculations were made. These indicated that beam spill should be contained within the cyclotron vault.

It should be noted, however, that the accuracy to which the program REVMOC was asked to predict beam spill is, at best, at the limit of the program. In normal use, one would expect an accuracy of 0.5% at best. Thus the quoted beam spills should be regarded as indications that spill might occur rather than an absolute value to be quoted.

A study of the effect of a vacuum window at the end of the beam line has been made. The results indicate that the window would increase the beam size by 2 mm in each of the horizontal and vertical planes. It is felt that this increase is reasonable and, in any event, the presence of the window is necessary. It is possible that the optics of the beam line could be modified to produce a smaller beam spot at the targets in the

TRANSPORT design such that in REVMOC simulations the nominal ± 2.5 mm goal is reached. This will be attempted at a later date.

References

1. G. M. Stinson, *TRIUMF report* TRI-DNA-96-5, TRIUMF, 1996.
2. K. L. Brown and S. K. Howry, *TRANSPORT/360*, SLAC-91, Stanford Linear Accelerator Laboratory, July, 1970.
3. C. J. Kost and P. A. Reeve, *TRIUMF report* TRI-DN-82-28, TRIUMF, 1982.
4. R. Lee, *Private communication*, October, 1965.
5. G. M. Stinson, *TRIUMF report* TRI-DNA-96-7, TRIUMF, 1996.
6. M. Dehnel, *TRIUMF report* TRI-DN-ISAC-16, TRIUMF, 1996.
7. A. J. Otter, *Private communication*, TRIUMF, June, 1996.

Table 1 (a)
Combination magnet parameters from ref²⁾

Parameter	480 MeV	490 MeV	500 MeV
Entry angle (°)	-0.977	-0.138	0.687
Field (kG)	1.726	0.248	-1.245
Exit angle (°)	0.000	0.000	0.000
Bend angle (°)	-0.977	-0.138	0.687

Table 1 (b)
Fringe field and initial beam parameters from ref²⁾

Parameter	400 MeV	450 MeV	500 MeV
$\pm x$ (cm)	0.127	0.127	0.127
$\pm \theta$ (mr)	1.600	1.600	1.600
$\pm y$ (cm)	0.669	0.669	0.669
$\pm \phi$ (mr)	0.556	0.556	0.556
R_{11} (cm/cm)	-0.03099	-0.01551	-0.06571
R_{12} (cm/mr)	0.32538	0.32610	0.32167
R_{16} (cm/%)	1.36150	1.32879	1.28344
R_{21} (mr/cm)	-3.09350	-3.06770	-3.17670
R_{22} (mr/mr)	0.16141	0.17049	0.16907
R_{26} (mr/%)	2.38040	2.43140	2.45410
R_{33} (cm/cm)	1.12700	1.11600	1.10800
R_{34} (mr/cm)	0.61980	0.61590	0.61200
R_{43} (mr/cm)	0.48200	0.46410	0.44710
R_{44} (cm/cm)	1.15300	1.15300	1.14900

Coordinates of the cross-over point of the combination magnet are:

$$R = 412.320 \text{ inches}$$

$$\theta = 327.000^\circ \text{ with respect to the centerline of valley 3}$$

Table 2

TRANSPORT listing for beam delivery of a 500 MeV beam to the west target (TGT2)

'DATA OF 95/10/10 on 96/09/30 - 500 MEV - TGT2 - 2AQ15 MOVED'

0					
13.00	', '	12.00000;			
16.00	'1/R1'	12.00000	0.00000;		
16.00	'1/R2'	13.00000	0.00000;		
16.00	'G/2 '	5.00000	5.08000;		
16.00	'X0 '	16.00000	-0.29135;		
16.00	'Z0 '	18.00000	11.07463;		
16.00	'T0 '	19.00000	35.10000;		
1.00	'BEAM'	0.12700	1.60000	0.66900	0.55600
		0.00000	0.10000	1.09007;	
12.00	'12 '	0.00000	0.00000	0.00000	0.00000
		0.00000	-0.96300	0.00000	0.00000
		0.00000	0.00000	0.00000	0.00000
		0.00000	0.00000	0.00000;	
1.00	'FOIL'	0.00000	0.17100	0.00000	0.17100
		0.00000	0.00000	0.00000	0.00000
14.00	'R1 '	-0.06571	0.32167	0.00000	0.00000
		0.00000	1.28344	1.00000;	
14.00	'R2 '	-3.17670	0.16907	0.00000	0.00000
		0.00000	2.45410	2.00000;	
14.00	'R3 '	0.00000	0.00000	1.10800	0.61200
		0.00000	0.00000	3.00000;	
14.00	'R4 '	0.00000	0.00000	0.44710	1.14900
		0.00000	0.00000	4.00000;	
3.00	'CMEX'	-0.59617;			
3.00	', '	0.21004;			
3.00	', '	0.30940;			
5.00	'2VQ1'	0.40900	-3.63609	5.08000;	
3.00	', '	0.25000;			
5.00	'2VQ2'	0.40900	5.21560	5.08000;	
3.00	', '	0.23880;			
3.00	'B1IN'	0.37190;			
20.00	', '	180.00000;			
2.00	', '	13.75000;			
4.00	'BEN1'	1.24595	14.00681	0.00000;	
2.00	', '	13.75000;			
20.00	', '	-180.00000;			
3.00	'B1EX'	0.00001;			
3.00	', '	0.08972;			
3.00	', '	0.27380;			
3.00	', '	0.52450;			
3.00	', '	0.27380;			

Table 2 (continued)

3.00	'B2IN'	0.08972;			
20.00	''	180.00000;			
2.00	''	13.75000;			
4.00	'BEN2'	1.24595	14.00681	0.00000;	
2.00	''	13.75000;			
20.00	''	-180.00000;			
3.00	'B2EX'	0.00001;			
-10.00	'ZFIT'	8.00000	3.00000	14.07160	0.00100;
3.00	''	1.00000;			
5.00	'2VQ3'	0.26600	5.61565	5.08000;	
3.00	''	0.28640;			
5.00	'2VQ4'	0.26600	-4.60155	5.08000;	
3.00	''	0.40900;			
3.00	''	0.28640;			
3.00	''	1.00000;			
3.00	''	1.00000;			
3.00	'WST1'	1.78321;			
-10.00	'FXW1'	2.00000	1.00000	0.00000	0.00100;
-10.00	'FYW1'	4.00000	3.00000	0.00000	0.00100;
-10.00	'SXW1'	1.00000	1.00000	1.15000	0.01000;
-10.00	'SYW1'	3.00000	3.00000	0.66000	0.01000;
3.00	''	1.00000;			
3.00	''	1.23290;			
5.00	'2VQ5'	0.26600	-1.66483	5.08000;	
3.00	''	0.28640;			
5.00	'2VQ6'	0.26600	3.12057	5.08000;	
3.00	''	0.28640;			
5.00	'2VQ7'	0.26600	-1.66483	5.08000;	
3.00	''	0.95770;			
3.00	'WALL'	1.51760;			
-10.00	'ZFIT'	8.00000	1.00000	15.24000	0.00100;
3.00	'MID2'	0.92100;			
3.00	'WALX'	1.36500;			
3.00	''	1.00000;			
3.00	''	1.00000;			
3.00	''	1.00000;			
3.00	''	1.00000;			
3.00	''	1.00000;			
3.00	''	1.00000;			
3.00	''	1.00000;			
3.00	''	1.00000;			
3.00	'WST2'	1.00000;			
-10.00	'FXW2'	2.00000	1.00000	0.00000	0.00100;
-10.00	'FYW2'	4.00000	3.00000	0.00000	0.00100;
3.00	''	1.00000;			
3.00	''	1.00000;			

Table 2 (continued)

3.00	,	1.00000;		
5.00	'2AQ8'	0.40900	-1.52363	5.08000;
3.00	,	0.30480;		
5.00	'2AQ9'	0.40900	2.63611	5.08000;
3.00	,	0.30480;		
5.00	'AQ10'	0.40900	-1.52363	5.08000;
3.00	,	0.96066;		
3.00	,	0.96066;		
3.00	,	1.04211;		
3.00	'WST3'	0.60000;		
-10.00	'FXW3'	2.00000	1.00000	0.00000
-10.00	'FYW3'	4.00000	3.00000	0.00000
-10.00	'SYW3'	3.00000	3.00000	0.29100
3.00	,	1.00000;		
3.00	,	1.00000;		
3.00	,	1.13330;		
5.00	'AQ11'	0.26600	2.32602	5.08000;
3.00	,	0.28640;		
5.00	'AQ12'	0.26600	-2.63114	5.08000;
3.00	,	1.13330;		
3.00	,	1.00000;		
3.00	'WST4'	1.00000;		
3.00	,	1.08328;		
3.00	,	1.08328;		
3.00	,	1.08328;		
3.00	,	1.07408;		
5.00	'AQ13'	0.26600	3.18591	5.08000;
3.00	,	0.28640;		
5.00	'AQ14'	0.26060	-3.51541	5.08000;
3.00	,	1.07408;		
3.00	,	1.08328;		
3.00	,	1.08328;		
3.00	'B3IN'	1.08328;		
16.00	'1/R2'	13.00000	1.73055;	
20.00	,	180.00000;		
2.00	,	7.50000;		
4.00	'BEN3'	0.68139	13.97007	0.00000;
2.00	,	7.50000;		
20.00	,	-180.00000;		
3.00	'B3EX'	0.00001;		
3.00	,	0.75000;		
3.00	,	0.74200;		
3.00	,	0.26600;		
3.00	'B4IN'	0.49200;		
16.00	'1/R2'	13.00000	0.00000;	

Table 2 (continued)

20.00	' '	180.00000;			
2.00	' '	7.50000;			
4.00	'BEN4'	0.68139	13.97007	0.00000;	
2.00	' '	7.50000;			
20.00	' '	-180.00000;			
3.00	'B4EX'	0.00001;			
3.00	' '	0.26500;			
3.00	' '	0.26500;			
3.00	' '	0.25580;			
5.00	'AQ15'	0.26600	4.85239	5.08000;	
3.00	' '	0.28640;			
5.00	'AQ16'	0.26600	-5.15018	5.08000;	
3.00	' '	0.32257;			
3.00	' '	0.88377;			
3.00	'YWST'	0.88377;			
-10.00	' '	4.00000	3.00000	0.00000	0.00100;
3.00	'TGT2'	0.88377;			
-10.00	' '	-1.00000	6.00000	0.06000	0.00100;
-10.00	' '	1.00000	1.00000	0.25000	0.01000;
-10.00	' '	3.00000	3.00000	0.25000	0.01000;
-10.00	'ZFIT'	8.00000	1.00000	57.91640	0.00100;
-10.00	'ZFIT'	8.00000	3.00000	10.85215	0.00100;

Table 3
Element settings as a function of energy for beam line 2A

Element	Field (kG) at energy					
	480 MeV	490 MeV	500 MeV			
2AVQ1	-3.55885	-3.59340	-3.63609			
2AVQ2	5.03422	5.09663	5.21560			
2AVB1	13.66610	13.83687	14.00681			
2AVB2	13.66610	13.83687	14.00681			
2AVQ3	5.53312	5.59629	5.61565			
2AVQ4	-4.54074	-4.58767	-4.60155			
2AVQ5	-1.59219	-1.61331	-1.66483			
2AVQ6	2.99027	3.03033	3.12057			
2AVQ7	-1.59219	-1.61331	-1.66483			
2AQ8	-1.47043	-1.49054	-1.52363			
2VQ9	2.54777	2.58248	2.63611			
2Q10	-1.47043	-1.49054	-1.52363			
2AQ11	2.25242	2.28376	2.32602			
2AQ12	-2.54611	-2.58129	-2.63114			
2AQ13 ^{a)}	3.13193	4.23486	3.17008	4.29335	3.18591	4.37081
2AQ14 ^{a)}	-3.44725	-4.08818	-3.48921	-4.14287	-3.51541	-4.21070
2AB3	13.63020		13.80052		13.97007	
2AB4	13.63020		13.80052		13.97007	
2AQ15 ^{a)}	4.71716	6.55437	4.77886	6.63379	4.85239	6.70106
2AQ15 ^{a)}	-5.02532	-5.84602	-5.08763	-5.91956	-5.15018	-5.99745

^{a)} Two field values are listed for quadrupoles 2AQ13 through 2AQ16. At a given energy, the left value refers to beam delivery to the target labelled TGT2 and the right to beam delivery to that labelled TGT1.

Table 4
Beam sizes at the waist locations

Waist	Parameter	480 MeV	490 MeV	500 MeV
WST1	$\pm x$ (cm)	1.150	1.150	1.182
	$\pm \theta$ (mr)	0.354	0.355	0.364
	$\pm y$ (cm)	0.660	0.660	0.661
	$\pm \phi$ (mr)	0.231	0.231	0.230
WST2	$\pm x$ (cm)	1.050	1.049	1.079
	$\pm \theta$ (mr)	0.387	0.389	0.339
	$\pm y$ (cm)	0.332	0.332	0.329
	$\pm \phi$ (mr)	0.459	0.459	0.461
WST3	$\pm x$ (cm)	1.047	1.046	1.076
	$\pm \theta$ (mr)	0.389	0.390	0.400
	$\pm y$ (cm)	0.294	0.293	0.291
	$\pm \phi$ (mr)	0.518	0.519	0.522
WST4	$\pm x$ (cm)	0.853	0.851	0.875
	$\pm \theta$ (mr)	0.477	0.479	0.492
	$\pm y$ (cm)	0.397	0.397	0.397
	$\pm \phi$ (mr)	0.383	0.383	0.383

Table 5(a)

Beam sizes and overall transfer matrices at the TGT2 location

Parameter	480 MeV	490 MeV	500 MeV
$\pm x$ (cm)	0.250	0.250	0.250
$\pm \theta$ (mr)	0.929	3.931	0.972
$\pm y$ (cm)	0.250	0.250	0.250
$\pm \phi$ (mr)	0.624	0.624	0.623
R_{11} (cm/cm)	-0.7029	-0.6958	-0.6866
R_{12} (cm/mr)	0.1453	0.1454	0.1456
R_{16} (cm/%)	-0.0006	0.0003	0.0001
R_{21} (mr/cm)	-5.2579	-5.2277	-5.1824
R_{22} (mr/mr)	-0.3383	-0.3419	-0.3731
R_{26} (mr/%)	3.4746	3.5108	3.8879
R_{33} (cm/cm)	-0.4510	-0.4475	-0.4530
R_{34} (mr/cm)	-0.0985	-0.0940	-0.1011
R_{43} (mr/cm)	-2.3011	-2.3047	-2.2969
R_{44} (cm/cm)	-2.7214	-2.7204	-2.7190

Table 5(b)

Beam sizes and overall transfer matrices at the TGT1 location

Parameter	480 MeV	490 MeV	500 MeV
$\pm x$ (cm)	0.250	0.250	0.250
$\pm \theta$ (mr)	2.473	2.480	3.547
$\pm y$ (cm)	0.250	0.250	0.250
$\pm \phi$ (mr)	0.624	0.624	0.623
R_{11} (cm/cm)	-0.0054	-0.0028	0.0372
R_{12} (cm/mr)	-0.1554	-0.1554	-0.1553
R_{16} (cm/%)	0.0001	0.0006	-0.0003
R_{21} (mr/cm)	6.4175	6.4057	6.7012
R_{22} (mr/mr)	-0.8228	-0.8237	-0.8138
R_{26} (mr/%)	-19.92276	-19.3231	-20.1184
R_{33} (cm/cm)	-0.3696	-0.3678	-0.3841
R_{34} (mr/cm)	0.0051	0.0074	-0.0131
R_{43} (mr/cm)	-2.3510	-2.3524	-2.3407
R_{44} (cm/cm)	-2.6750	-2.6743	-2.6820

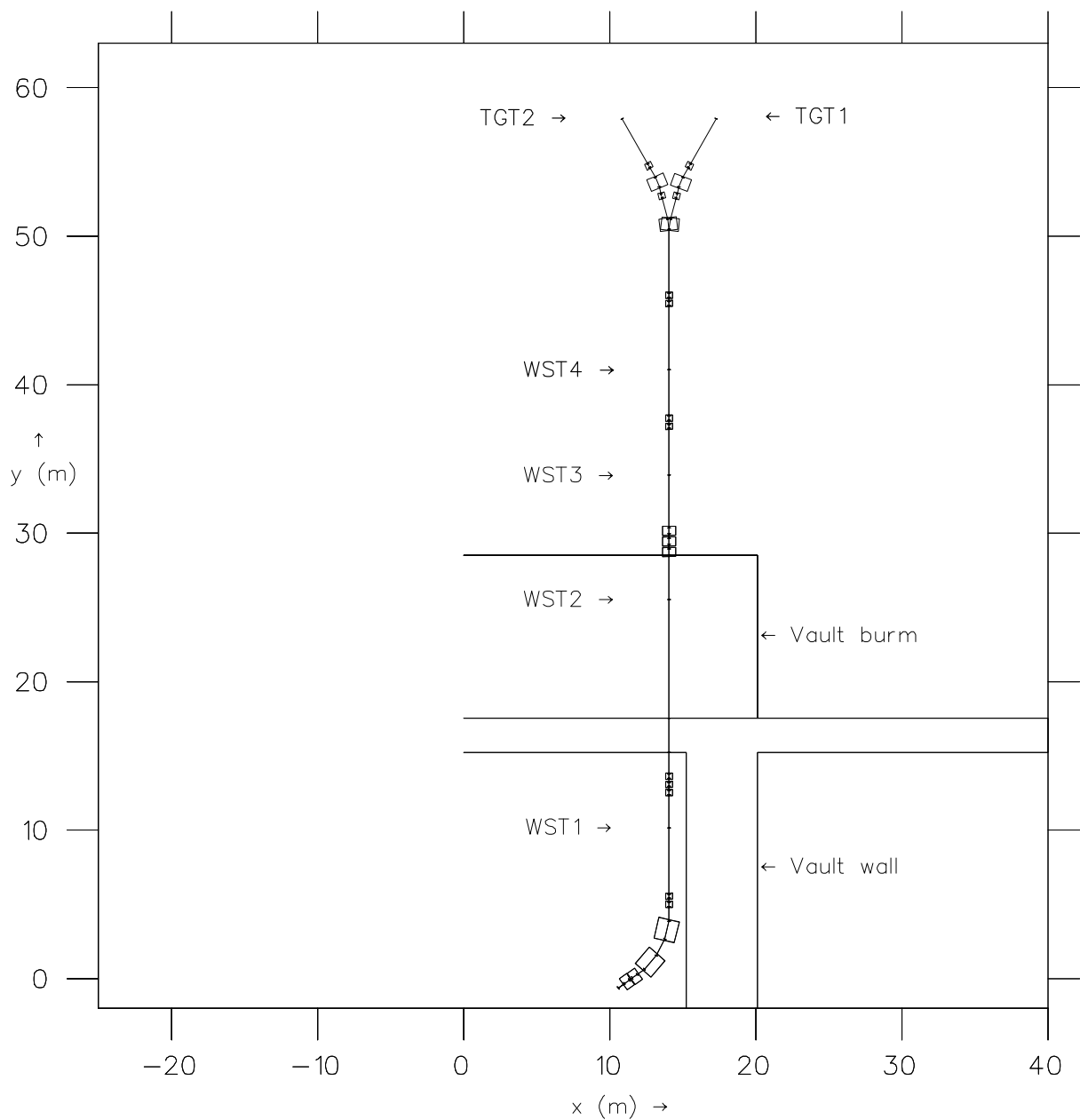


Figure 1. The configuration of beam line 2A given in ref¹.

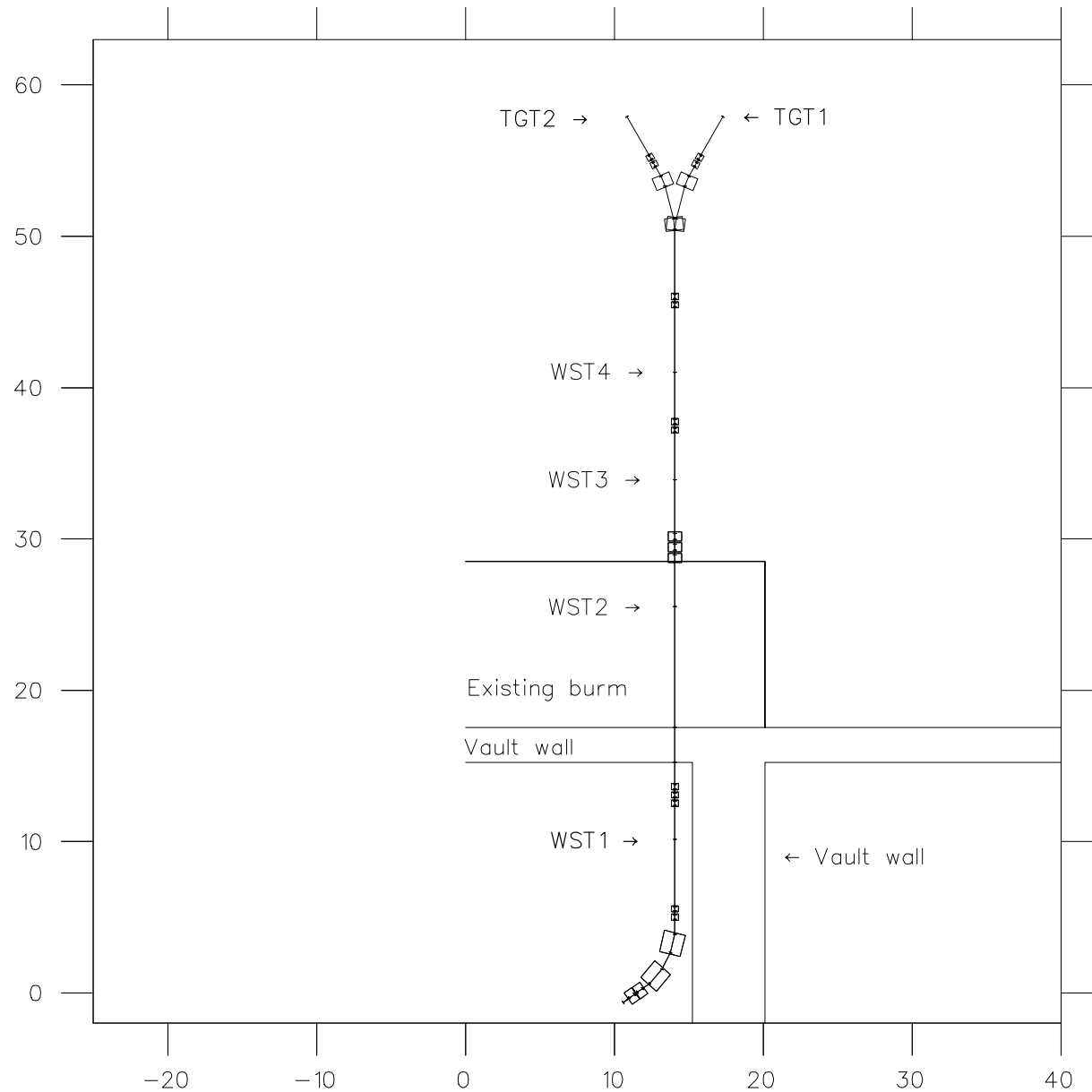


Figure 2. The proposed configuration of beam line 2A.

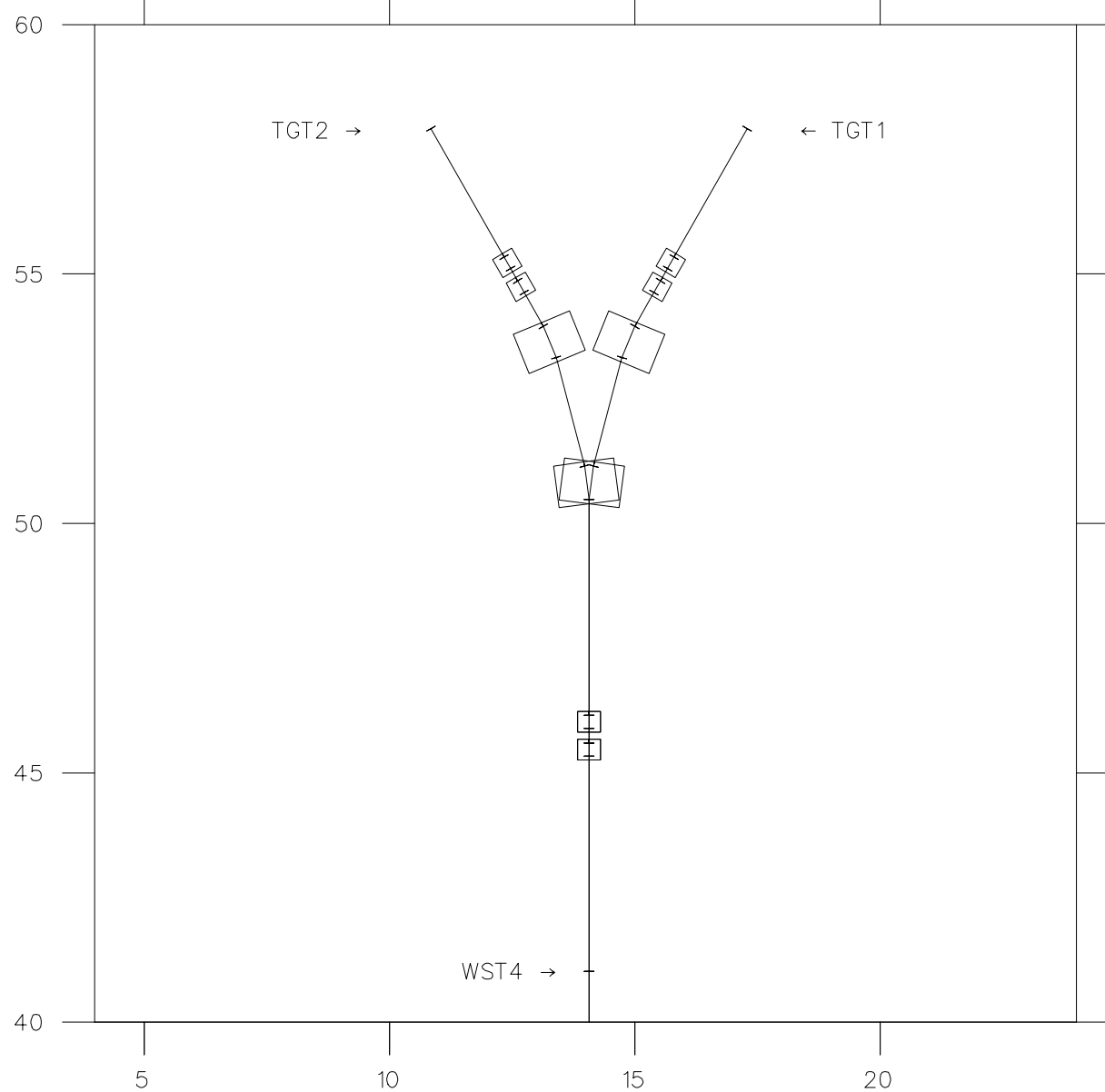


Figure 3. An enlarged view of the WST4 to target region of beam line 2A.

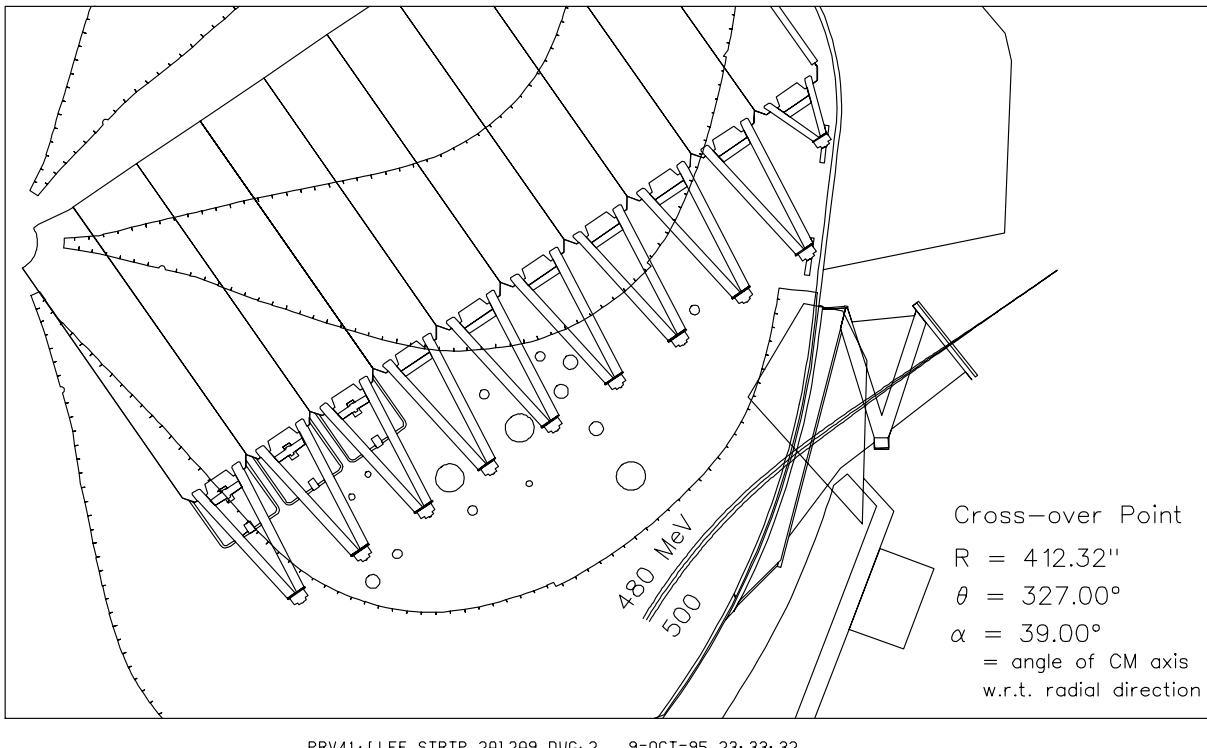


figure 4(a). The extraction trajectories for energies of 480, 490 and 500 MeV.

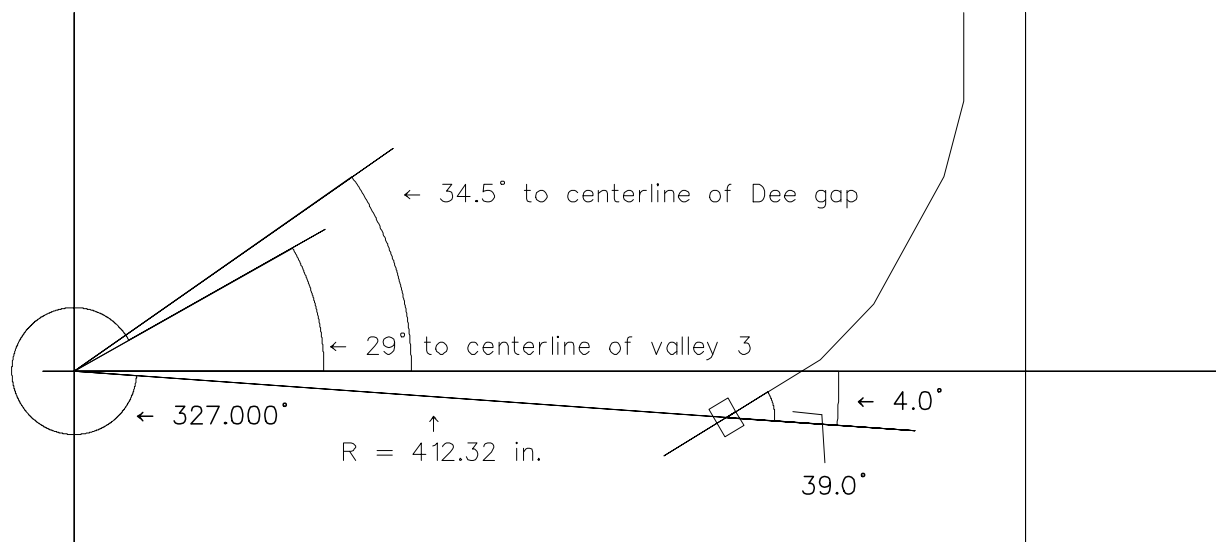


Figure 4(b). The essential geometry of beam line 2A extraction.

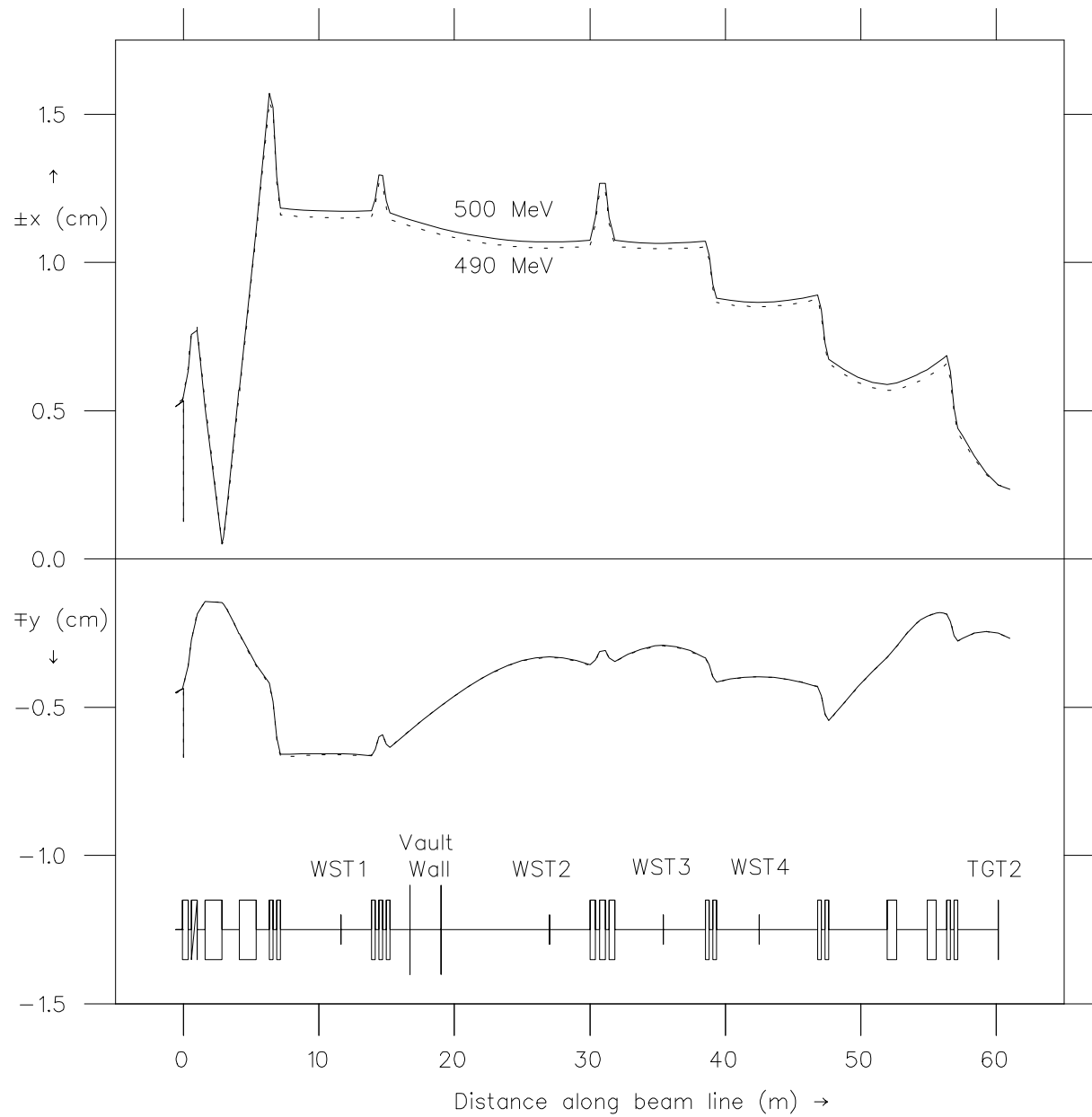


Figure 5. Beam envelopes along beam line 2A—beam delivery to TGT2.

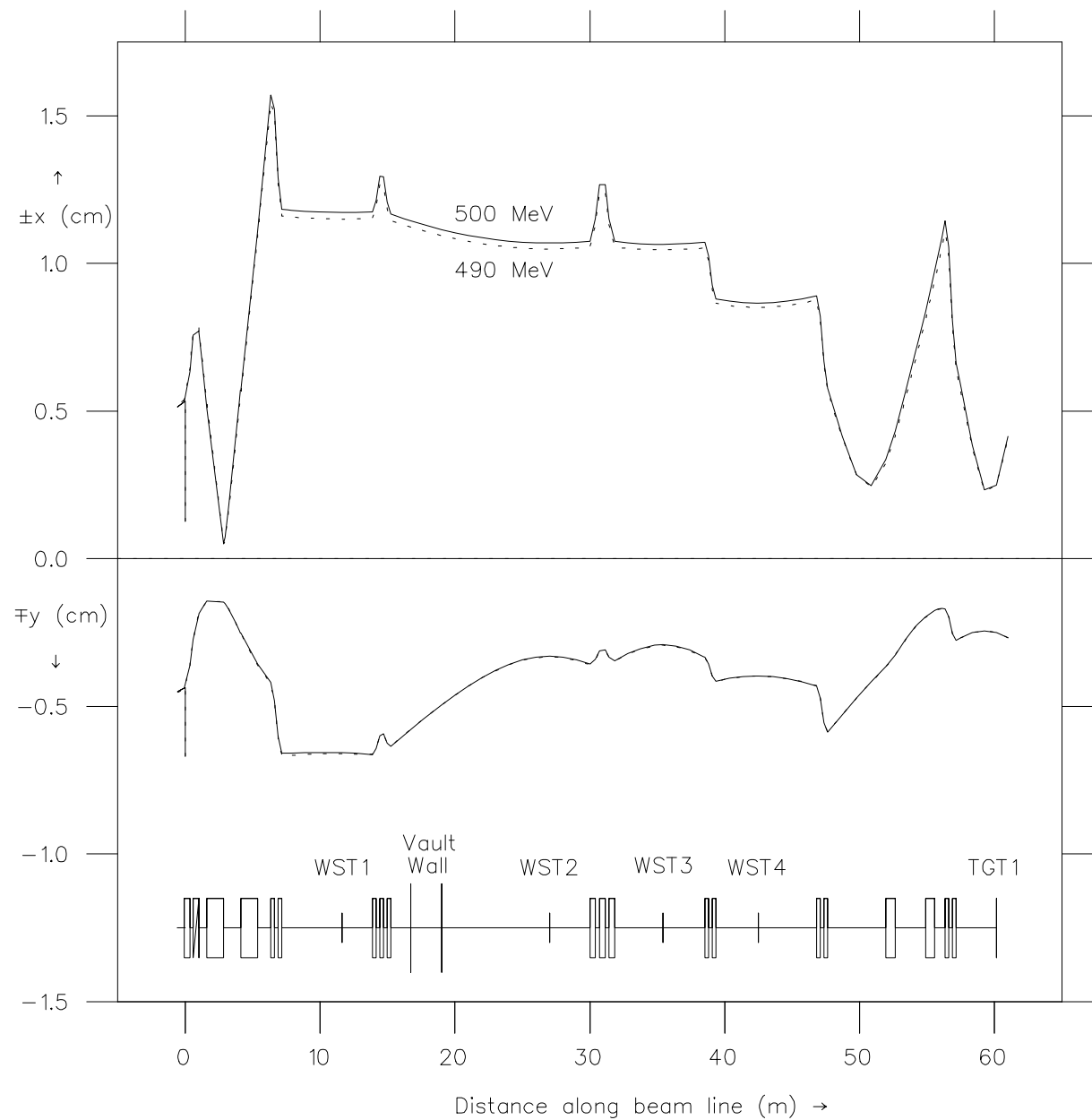


Figure 6. Beam envelopes along beam line 2A—beam delivery to TGT1.

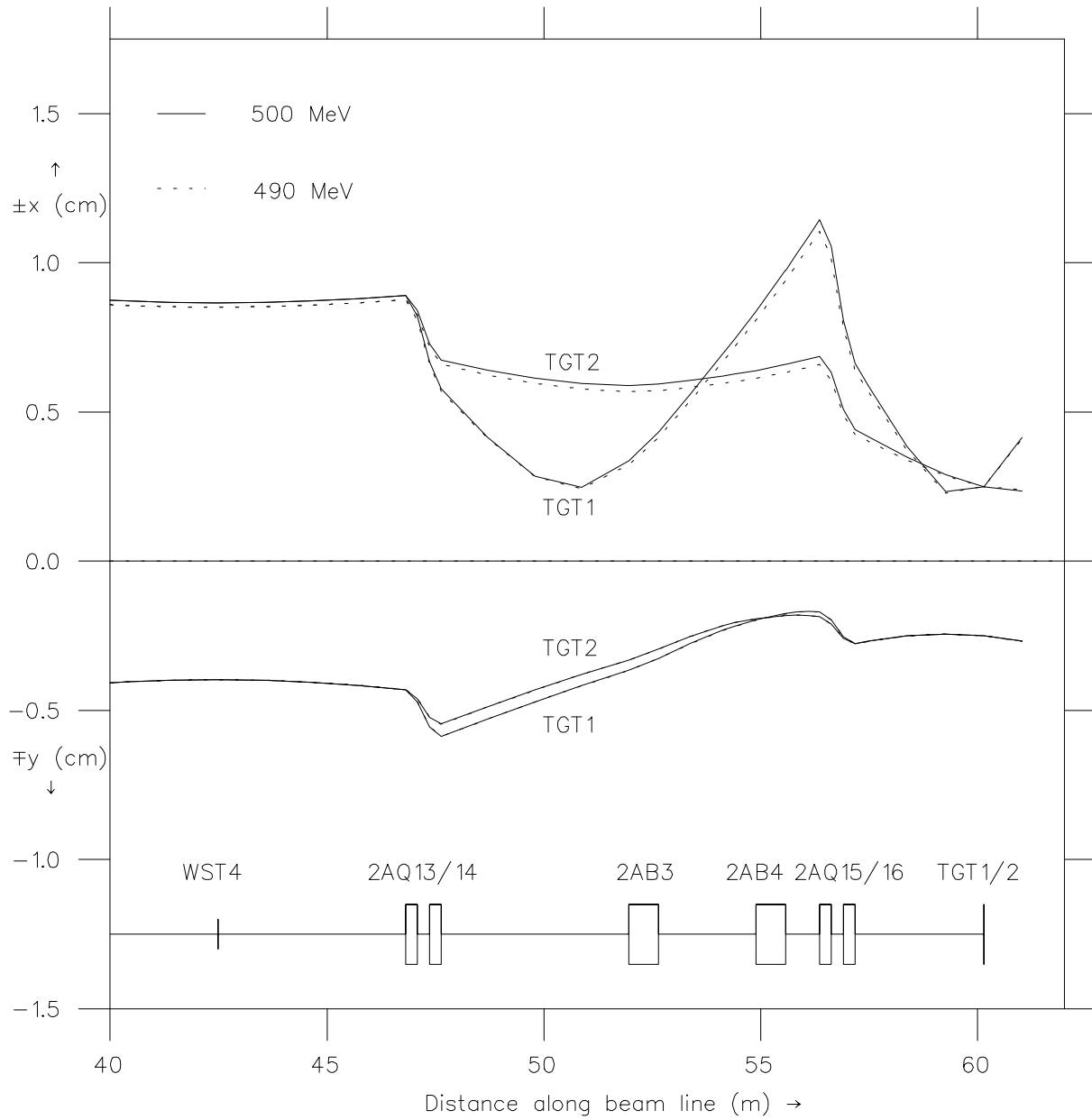


Figure 7. Enlarged beam profiles between WST4 and TGT1/2 locations on beam line 2A.

Figure 8. Predicted $\phi - y$ correlation at the WST1 location on beam line 2A.

DATA OF 95/10/10 ON 96/06/25 - 500 MEV ON 2-A - MOVE Q15 - 2xWst @ WST1 - TGT2 - Y WAIST 0.9 M UPSTREAM OF TGT

Space # 3: Distribution of particles as a function of X AT TGT2 (Element #149) (along HORIZONTAL axis)
 & Y at TGT2 (Element #149) (along VERTICAL axis)

REAL! Distribution of FINAL RUN FOUND HERE

COUNTS = 149986.

X PROJECTION

Figure 9. Predicted beam spot at the TGT2 location at 500 MeV.

Figure 10. Predicted beam spot at the TGT1 location at 500 MeV.

DATA OF 95/10/10 ON 96/09/30 - 490 MEV ON 2-A - MOVE Q15 - 2xWst @ WST1 - TGT2 - Y WAIST 0.9M UPSTREAM OF TGT

Space # 3: Distribution of particles as a function of X AT TGT2 (Element #149) (along HORIZONTAL axis)
& Y at TGT2 (Element #149) (along VERTICAL axis)

REAL! Distribution of FINAL RUN FOUND HERE

COUNTS = 149986.

X PROJECTION

Figure 11. Predicted beam spot at the TGT2 location at 490 MeV.

Figure 12. Predicted beam spot at the TGT1 location at 490 MeV.

DATA OF 95/10/10 ON 96/09/30 - 480 MEV ON 2-A - MOVE Q15 - 2xWst @ WST1 - TGT2 - Y WAIST 0.9M UPSTREAM OF TGT1

Space # 3: Distribution of particles as a function of X AT TGT2 (Element #148) (along HORIZONTAL axis)
 & Y at TGT2 (Element #148) (along VERTICAL axis)

REAL! Distribution of FINAL RUN FOUND HERE

COUNTS = 149984.

X PROJECTION

Figure 13. Predicted beam spot at the TGT2 location at 480 MeV.

Figure 14. Predicted beam spot at the TGT1 location at 480 MeV.

DATA OF 95/10/10 ON 96/06/25 - 500 MEV ON 2-A - MOVE Q15 - 2xWst @ WST1 - TGT2 - Y WAIST 0.9 M UPSTREAM OF TGT

Space # 5: Distribution of particles as a function of X AT TGT2 (Element #149) (along HORIZONTAL axis)
& P at TGT2 (Element #149) (along VERTICAL axis)

REAL! Distribution of FINAL RUN FOUND HERE

COUNTS = 149986.

X PROJECTION

Figure 15. Predicted correlation of momentum and horizontal position at the TGT2 location at 500 MeV.

DATA OF 95/10/10 ON 96/09/26 - 500 MEV - MOVE 2AQ15 - 0.001" SS 1.0 M UPSTREAM

Space #3: Distribution of particles as a function of X AT TGT2 (Element #152) (along HORIZONTAL axis)
 & Y at TGT2 (Element #152) (along VERTICAL axis)

REAL! Distribution of FINAL RUN FOUND HERE

COUNTS = 149944.

X PROJECTION

Figure 16. Predicted beam spot at the TGT2 location at 500 MeV including foil and window scattering.